THE JOURNAL OF BIOLOGICAL CHEMISTRY VOL. 281, NO. 30, pp. 21062–21072, July 28, 2006

Translesion Synthesis across Bulky N^2-Alkyl Guanine DNA Adducts by Human DNA Polymerase κ*[S]

Received for publication, March 9, 2006, and in revised form, April 6, 2006 Published, JBC Papers in Press, June 1, 2006, DOI 10.1074/jbc.M602246200

Jeong-Yun Choi[‡§], Karen C. Angel[‡], and F. Peter Guengerich[‡1]

From the [‡]Department of Biochemistry and Center in Molecular Toxicology, Vanderbilt University School of Medicine, Nashville, Tennessee 37232-0146 and the [§]Department of Pharmacology, College of Medicine, Ewha Womans University, 911-1 Mok-6-Dong, Yangcheon-Gu, Seoul 158-710, Republic of Korea

DNA polymerase (pol) κ is one of the so-called translesion polymerases involved in replication past DNA lesions. Bypass events have been studied with a number of chemical modifications with human pol κ, and the conclusion has been presented, based on limited quantitative data, that the enzyme is ineffective at incorporating opposite DNA damage but proficient at extending beyond bases paired with the damage. Purified recombinant full-length human pol κ was studied with a series of eight N^2-guanyl adducts (in oligonucleotides) ranging in size from methyl- to -CH_2(6-benzo[*a*]pyrenyl) (BP). Steady-state kinetic parameters (catalytic specificity, k_{cat}/K_m) were similar for insertion of dCTP opposite the lesions and for extension beyond the N^2-adduct G:C pairs. Mispairing of dGTP and dTTP was similar and occurred with k_{cat}/K_m values ~10^{-3} less than for dCTP with all adducts; a similar differential was found for extension beyond a paired adduct. Pre-steady-state kinetic analysis showed moderately rapid burst kinetics for dCTP incorporations, even opposite the bulky methyl(9-anthracenyl)- and BPG adducts (k_p 5.9–10.3 s^{-1}). The rapid bursts were abolished opposite BPG when α-thio-dCTP was used instead of dCTP, implying rate-limiting phosphodiester bond formation. Comparisons are made with similar studies done with human pols η and ι; pol κ is the most resistant to N^2-bulk and the most quantitatively efficient of these in catalyzing dCTP incorporation opposite bulky guanine N^2-adducts, particularly the largest (N^2-BPG).

DNA is constantly damaged by chemical and physical agents. When the damage is not repaired it can contribute to genomic instability and probably to several maladies, including cancer, cardiovascular disease, and aging (1, 2). Basic issues involved in the understanding of the etiology of mutation include the biochemical formation of electrophiles and oxygen radicals, characterization of their interactions with DNA, the enzymatic repair of damage, and the processing of DNA to generate permanent changes in the genetic information. In this latter regard, the enzymology of DNA replication is of considerable interest.

The mutation of DNA cannot be understood only in the context of preferred base pairing, in that the free energy differences among various pairs of natural and modified DNA bases are not sufficient to explain normal or abnormal pairing (3). Thus, the major driving forces in the generation of mutations from damaged DNA are the polymerases (4). The normal replicative DNA polymerases are the first that encounter DNA adducts, and some small DNA adducts (*e.g.* O^6-MeG and 8-oxo-7,8-dihydroG)[2] are processed by these polymerases, at least part of the time. However, a group of DNA polymerases first discovered in the late 1990s participates in "translesion" synthesis beyond small and large DNA adducts, although the process is, in general, less efficient and more error-prone than the reactions that replicative polymerases catalyzed with unmodified DNA (1, 5).

One of these "Y-family" translesion polymerases is polymerase (pol) κ, studied in mammals. pol κ was discovered as a homolog of the *Escherichia coli din*B gene product (pol IV), an enzyme involved in the SOS adaptive response (6, 7). The crystal structure of a core element of human pol κ has been determined (8). The ability of pol κ to bypass a number of types of DNA damage has been reported, including guanine modified with *N*-acetylaminofluorene or BPDE (9–14), xanthine (15), 8-nitroguanine (16), and guanine modified with oxidized estrogens (17). However, pol κ has not been judged to be very efficient in bypassing UV photoproducts (9, 18), *cis*-platin-modified DNA (10), 1,N^6-ethenodeoxyadenine (19), O^6-MeG (20), or 8-(hydroxymethyl)-3,N^4-ethenoC (21). Other issues involving pol κ include up-regulation in lung cancer (22), a possible (but not established) role in somatic hypermutation (23), and a general role in genome maintenance *versus* instability (24).

A case has been made that pol κ acts mainly as an "extender" of damaged DNA that has already undergone insertions opposite modified bases, as opposed to a role in misinsertion itself (20, 25, 26). Few of the studies on pol κ provide very much

* This work was supported by United States Public Health Services Grants R01 ES10375 and P30 ES00267 (to F. P. G.). The costs of publication of this article were defrayed in part by the payment of page charges. This article must therefore be hereby marked "*advertisement*" in accordance with 18 U.S.C. Section 1734 solely to indicate this fact.

[S] The on-line version of this article (available at http://www.jbc.org) contains SDS-polyacrylamide gel electrophoretic analysis of purified DNA polymerase κ (supplemental Figs. S1 and S2).

[1] To whom correspondence should be addressed: Dept. of Biochemistry and Center in Molecular Toxicology, Vanderbilt University School of Medicine, 638 Robinson Research Bldg., 23rd and Pierce Avenues, Nashville, TN 37232-0146. Tel.: 615-322-2261; Fax: 615-322-3141; E-mail: f.guengerich@vanderbilt.edu.

[2] The abbreviations used are: Me, methyl; Et, ethyl; Ib, isobutyl; Bz, benzyl; N^2-Naph, N^2-CH_2(2-naphthyl); N^2-Anth, N^2-CH_2(9-anthracenyl); N^2-BP, N^2-CH_2(6-benzo[*a*]pyrenyl); BPDE, benzo[*a*]pyrene diol epoxide; dCTPαS, 2′-deoxycytidine 5′-*O*-(1-thiotriphosphate); PCNA, proliferating cell nuclear antigen; pol, DNA polymerase; RT, reverse transcriptase; $T7^-$, bacteriophage DNA polymerase T7, exonuclease-deficient; HIV-1, human immunodeficiency virus, type 1.

quantitative information about catalysis of either misinsertion as further extension. Some steady-state kinetic studies have been done, but many only report steady-state rates as percentages and cannot be converted to k_{cat} values. Also, after applying some assumptions about the actual enzyme concentrations used, many of the rates appear to be very low. Even if valid steady-state kinetic analyses are reported, their usefulness is limited by the complexity of the polymerase catalytic cycle (27).

To obtain a better perspective on the role of human pol κ, we prepared a purified full-length enzyme and utilized this in kinetic and other studies with a defined oligonucleotide containing a G or each of eight N^2-substituted Gs at the same site. Thus, the system varies only in the size of the lesion (with associated changes in hydrophobicity and electronic properties), and the results obtained with pol κ can be compared directly with corresponding studies done with HIV-1 RT and bacteriophage T7$^-$ (28) and two other human Y-family polymerases, pol η (29) and pol ι (30). Our results indicate that pol κ is particularly resilient to blockage with the larger adducts, as judged by several criteria, and that incorporation opposite the adducts is as efficient as extension.

EXPERIMENTAL PROCEDURES

Materials—Unlabeled dNTPs were obtained from Amersham Biosciences, (S_p)-dCTPαS was from Biolog Life Science Institute (Bremen, Germany), and [γ-^{32}P]ATP (specific activity 3×10^3 Ci mmol^{-1}) was from PerkinElmer Life Sciences. T4 polynucleotide kinase and restriction endonucleases were purchased from New England Biolabs (Beverly, MA). Bio-spin columns were obtained from Bio-Rad. A protease inhibitor mixture (mixture) was from Roche Applied Science (Indianapolis, IN). Human testis cDNA was purchased from BD Biosciences Clontech (Palo Alto, CA). *Pfu ultra* DNA polymerase and pPCR-Script Amp vector were purchased from Stratagene (La Jolla, CA). BaculoGold transfection kits were obtained from BD Biosciences Pharmingen (San Diego, CA). Amicon Ultra centrifugal filter devices were purchased from Millipore (Billerica, MA).

Oligonucleotides—Unmodified 24-mer, 25-mers, and 36-mer (Table 1) were purchased from Midland Certified Reagent Co. (Midland, TX). Eight 36-mers, each containing a guanine N^2-adduct (N^2-MeG, N^2-EtG, N^2,N^2-diMeG, N^2-IbG, N^2-BzG, N^2-NaphG, N^2-AnthG, and N^2-BPG) were prepared as previously described and characterized by capillary gel electrophoresis and matrix-assisted laser desorption ionization/time-of-flight mass spectrometry (28–30). The extinction coefficients for the oligonucleotides, estimated by the Borer method (31) were as follows: 24-mer, $\epsilon_{260} = 224$ mM^{-1} cm^{-1}; 25-mer, $\epsilon_{260} = 232$ mM^{-1} cm^{-1}; and 36-mer, $\epsilon_{260} = 310$ mM^{-1} cm^{-1} (28, 29).

Isolation of Human POLK cDNA and Construction of Recombinant Baculovirus—Human DNA polymerase κ cDNA was obtained by PCR amplification from human testis cDNA (as template) using *Pfu ultra* DNA polymerase with the corresponding two primers 5′-CTCGAGGCATGGATAGCACAAAGGA-3′ and 5′-GGATTATTGCACTTGCCTTCA-3′. The resulting 2.7-kb PCR product of *POLK* was cloned into the vector pPCR-Script Amp, and nucleotide sequencing was used to confirm the entire sequence of the coding region. The fragment containing the human *POLK* gene was cloned into the vector pAcHLT-B using the XhoI and NotI sites to generate a fusion tag containing six histidines at the N terminus, yielding the vector pAcHLT/HPOLK. The plasmid was co-transfected into Sf9 insect cells using BaculoGold DNA (with a BaculoGold transfection kit) to generate the recombinant baculovirus expressing human pol κ.

Expression and Purification of Human DNA Polymerases—Recombinant human pol κ P3 viral stocks were used to infect 600-ml spinner flask cultures of Sf9 cells at 1×10^6 cells ml^{-1}. The infected cells were incubated for 60 h and harvested by centrifugation for 10 min at 4 °C at $3 \times 10^3 \times g$. Cells were resuspended in 50 ml of Buffer A (50 mM Tris-HCl (pH 7.5), 500 mM NaCl, 5 mM 2-mercaptoethanol, and 10% (v/v) glycerol) containing 0.5% (v/v) Nonidet P-40 and Roche Complete protease inhibitor mixture (one tablet per 50 ml). Cell debris was pelleted by ultracentrifugation for 60 min at 4 °C at $10^5 \times g$. The resulting supernatant was loaded (0.3 ml min^{-1}) onto a 5-ml HisTrap HP affinity column (Amersham Biosciences) in an Amersham Biosciences Δkta fast-protein liquid chromatography system at 4 °C. The column was washed (at 0.8 ml min^{-1}) with 50 ml of Buffer A containing 20 mM imidazole, 50 ml of Buffer A containing 40 mM imidazole, and then with 50 ml of Buffer A containing 50 mM imidazole. Bound enzyme was eluted with 400 mM imidazole (in Buffer A). Fractions containing pol κ were collected, diluted 5-fold with Buffer B (50 mM Tris-HCl (pH 7.5), 10% glycerol (v/v), 5 mM 2-mercaptoethanol, and 1 mM EDTA), and loaded onto a 1-ml Mono S column (Amersham Biosciences). Unbound protein was washed from the column with 20 ml of Buffer B containing 350 mM NaCl, and pol κ was eluted with a 30-ml linear gradient of 0.35 to 2 M NaCl in Buffer B. Eluted fractions (0.26 ml) were analyzed by SDS-polyacrylamide gel electrophoresis with silver staining (32). pol κ was found to be eluted at 600 mM NaCl. Pooled fractions were concentrated using an Amicon Ultra centrifugal filter (Millipore) to a volume of 100 μl and further purified to near homogeneity using a Superdex 200 column (Amersham Biosciences) with Buffer B containing 150 mM NaCl. Fractions containing >95% pure recombinant protein were pooled, concentrated, and exchanged into storage buffer (50 mM Tris-HCl, pH 7.5, 50% glycerol (v/v), 1 mM dithiothreitol, and 1 mM EDTA). The active enzyme concentration of pol κ was determined by the active site titration method (see below).

Recombinant human pol δ was prepared as described previously (29). Recombinant human PCNA was prepared in *E. coli* and purified as described (33, 34).

Reaction Conditions for Enzyme Assays—Standard DNA polymerase reactions were done in 50 mM Tris-HCl (pH 7.5) buffer containing 5 mM dithiothreitol, 100 μg bovine serum albumin ml^{-1} (w/v), and 10% glycerol (v/v) with 100 nM primer-template at 37 °C (28–30). Primers were 5′ end-labeled using T4 polynucleotide kinase/[γ-^{32}P]ATP and annealed with template (36-mer). All reactions were initiated by the addition of dNTP solutions containing $MgCl_2$ (5 mM final concentration) to preincubated enzyme/DNA mixtures.

Primer Extension Assay with All Four dNTPs ("Run-on" or "Standing Start" Experiments)—A ^{32}P-labeled primer, annealed to either an unmodified or modified (N^2-alkylG) template, was

extended in the presence of all four dNTPs (100 μM each) for 15 min. Reaction mixtures (8 μl) were quenched with 2 volumes of a solution of 20 mM EDTA in 95% formamide (v/v) (28). Products were resolved using a 16% polyacrylamide (w/v) gel electrophoresis system containing 8 M urea and visualized using a Bio-Rad Molecular Imager FX and Quantity One software (Bio-Rad).

Steady-state Kinetic Analyses—A ^{32}P-labeled primer, annealed to either an unmodified or adducted template, was extended in the presence of varying concentrations of a single dNTP. The molar ratio of primer/template complex to enzyme was at least 10:1. Polymerase concentrations and reaction times were chosen so that maximal product formation was ≤20% of the substrate concentration (35). The primer-template was extended with dNTP in the presence of 0.05–10 nM pol κ for 5 or 10 min. All reactions (8 μl) were done at ten dNTP concentrations (in duplicate) and quenched with 2 volumes of a solution of 20 mM EDTA in 95% formamide (v/v) (28–30). Products were resolved using a 16% polyacrylamide (w/v) electrophoresis gel containing 8 M urea and quantitated by phosphorimaging analysis using a Bio-Rad Molecular Imager FX instrument and Quantity One software. Graphs of product formation *versus* dNTP concentration were fit using nonlinear regression (hyperbolic fits) in GraphPad Prism Version 3.0 (San Diego, CA) for the determination of k_{cat} and K_m values.

Pre-steady-state Reactions—Rapid quench experiments were performed using a model RQF-3 KinTek Quench Flow Apparatus (KinTek Corp., Austin, TX). Reactions were initiated by rapid mixing of ^{32}P-primer/template/pol κ mixtures (12.5 μl) with the dNTP·Mg^{2+} complex (10.9 μl) and then quenched with 0.3 M EDTA after times varying from 10 ms to 2 s (or 4 s for N^2-BPG-containing DNA). Reaction products were mixed with 450 μl of formamide-dye solution (20 mM EDTA, 95% formamide (v/v), 0.5% bromphenol blue (w/v), and 0.05% xylene cyanol (w/v)) and separated using a denaturing electrophoresis gel, with quantitation as described for the steady-state reactions. Pre-steady-state experiments were fit with the burst equation $y = A(1 - e^{-k_p t}) + k_{ss}t$, where y = concentration of product, A = burst amplitude, k_p = pre-steady-state rate of nucleotide incorporation, t = time, and k_{ss} = steady-state rate of nucleotide incorporation (not normalized for enzyme concentration in the equation) (36, 37), using nonlinear regression analysis in GraphPad Prism Version 3.0.

Phosphorothioate Analysis—With the ^{32}P-primer annealed to either an unmodified or adducted template, reactions were initiated by rapid mixing of ^{32}P-primer/template/pol κ mixtures (12.5 μl) with (S_p)-dCTPαS·Mg^{2+} complex (or dCTP·Mg^{2+}) (10.9 μl) and then quenched with 0.3 M EDTA after reaction times varying from 10 ms to 2 s (or 4 s for N^2-BPG-containing DNA). Products were analyzed as described for the pre-steady-state reactions (see above).

Active Site Titration and Determination of K_d^{DNA}—The K_d^{DNA} for productive binding of pol κ to 24-mer/36-mer DNA substrates was determined using pre-steady-state analysis. pol κ (preincubated with increasing concentrations of the DNA substrate in sample syringe A) was mixed with a saturating concentration of dCTP·Mg^{2+}, from sample syringe B, and then quenched with 0.3 M EDTA after a time interval of 0.2 s. A graph of the burst amplitude *versus* total DNA concentration was plotted and fit to a quadratic equation, $A = 0.5(K_d + E_t + D_t) - [0.25(K_d + E_t + D_t)^2 - E_tD_t]^{1/2}$, where A = burst amplitude, E_t = active enzyme concentration, D_t = DNA concentration, and K_d = equilibrium dissociation constant for productive DNA binding (36, 37) in GraphPad Prism Version 3.0.

Determination of K_d^{dCTP}—K_d^{dCTP} was estimated by performing pre-steady-state reactions at different dNTP concentrations with reaction times varying from 10 ms to 2 s. A graph of the burst rate (k_{obs}) *versus* dCTP concentration was fit to the hyperbolic equation $k_{obs} = [k_{pol}[dNTP]/([dNTP] + K_d)]$, where k_{pol} = maximal rate of nucleotide incorporation and K_d^{dCTP} = equilibrium dissociation constant for dCTP (36, 37).

TABLE 1
Oligodeoxynucleotides used in this study

24-mer	5′-GCCTCGAGCCAGCCGCAGACGCAG
25C-mer	5′-GCCTCGAGCCAGCCGCAGACGCAGC
25T-mer	5′-GCCTCGAGCCAGCCGCAGACGCAGT
36-mer	3′-CGGAGCTCGGTCGGCGTCTGCGTC**G**[a]CTCCTGCGGCT

[a] **G** = G, N^2-MeG, N^2-EtG, N^2,N^2-diMeG, N^2-IbG, N^2-BzG, N^2-NaphG, N^2-AnthG, or N^2-BPG.

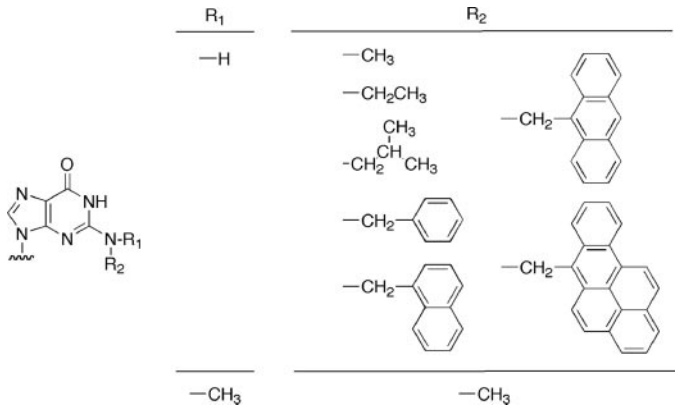

FIGURE 1. ***N^2*-Guanine derivatives used with pol κ.**

RESULTS

Overall Strategy—The goal of the research was to characterize the interactions of pol κ with damaged DNA and compare these with other human translesion DNA polymerases, particularly pols η and ι. Full-length human pol κ was prepared (see "Experimental Procedures" and Supplemental Fig. S1) and used in a series of quantitative steady-state and pre-steady-state kinetic measurements with a set of oligonucleotides in which a single G was substituted at the N2 atom with a series of adducts varying only in size (Table 1 and Fig. 1). Thus, the only variable involved in this comparison is the adduct size (although the electronic properties and hydrophobicity (30) of alkyl and aryl groups should not be ignored, in the context of base stacking (4)). Similar studies have been done with the replicative DNA polymerases HIV-1 RT and bacteriophage pol T7 (*exo*−) (28) and human pol η (29) and pol ι (30), and comparison of the properties of these three major human translesion DNA polymerases is now possible.

Primer Extension by Human pol κ Using All Four dNTPs—The first set of studies involved extension of the primer in the presence of all four dNTPs when paired with a template containing either a G or an N^2-alkylG (fixed incubation time and

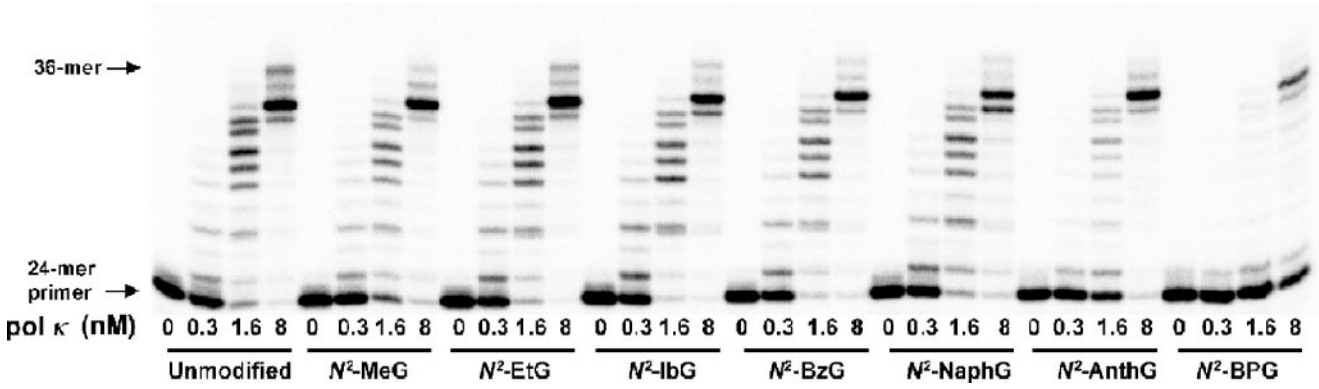

FIGURE 2. **Extension of ^{32}P-labeled primers opposite G, N^2-MeG, N^2-EtG, N^2-IbG, N^2-BzG, N^2-NaphG, N^2-AnthG, and N^2-BPG by human pol κ with all four dNTPs present.** A primer (24-mer) was annealed with each of the eight different 36-mer templates (Table 1) containing an unmodified G or N^2-modified G placed at the 25th position from the 3′-end. Reactions were done for 15 min with increasing concentrations of pol κ (0–8 nM) and 100 nM DNA substrate (primer/template) as indicated. The ^{32}P-labeled 24-mer primer was extended in the presence of all four dNTPs. Reaction products were resolved by denaturing gel electrophoresis with subsequent phosphorimaging analysis.

TABLE 2
Steady-state kinetic parameters for one-base incorporation by human pol κ

Template	dNTP	K_m	k_{cat}	k_{cat}/K_m	*f*
		μM	s^{-1}	$mM^{-1}\ s^{-1}$	*Misinsertion ratio*
G	C	8.4 ± 0.9	0.31 ± 0.01	37	1
	G	1300 ± 300	0.036 ± 0.003	0.028	0.0008
	T	6800 ± 700	0.38 ± 0.02	0.056	0.0015
N^2-MeG	C	11 ± 0.7	0.13 ± 0.01	12	1
	G	700 ± 60	0.044 ± 0.001	0.063	0.0053
	T	6000 ± 1000	0.29 ± 0.03	0.048	0.0041
N^2-EtG	C	22 ± 2	0.36 ± 0.01	16	1
	G	860 ± 160	0.023 ± 0.002	0.027	0.0016
	T	1600 ± 600	0.15 ± 0.03	0.094	0.0057
N^2-IbG	C	11 ± 1	0.66 ± 0.01	60	1
	G	330 ± 60	0.027 ± 0.001	0.082	0.0014
	T	1600 ± 600	0.17 ± 0.04	0.11	0.0018
N^2-BzG	C	6.2 ± 0.5	0.38 ± 0.01	61	1
	G	220 ± 20	0.12 ± 0.001	0.55	0.0090
	T	410 ± 80	0.045 ± 0.003	0.11	0.0018
N^2-NaphG	C	11 ± 1	0.27 ± 0.01	25	1
	G	460 ± 90	0.087 ± 0.006	0.19	0.0078
	T	870 ± 140	0.17 ± 0.01	0.20	0.0082
N^2-AnthG	C	47 ± 9	0.24 ± 0.01	5.1	1
	G	320 ± 60	0.0017 ± 0.0001	0.0053	0.0010
	T	890 ± 160	0.0080 ± 0.0007	0.0089	0.0017
N^2-BPG	C	32 ± 3	0.045 ± 0.001	1.4	1
	G	390 ± 80	0.0021 ± 0.0001	0.0053	0.0038
	T	760 ± 120	0.0063 ± 0.0004	0.0082	0.0059

varying concentrations of pol κ) (Fig. 2). Although PCNA has been reported to stimulate pol κ activity (38), it was only apparent in the presence of other accessory factors, *i.e.* replication factor C and replication protein A, with long and end-closed DNA templates (*e.g.* M13 circular template or 75-mer templates containing biotin-streptavidin complex at both ends), suggesting the different mechanism of stimulation (from pol δ, which can be stimulated by PCNA only). Gerlach *et al.* (10) did not observe direct stimulation nor did we in the preliminary experiments with these adducts, and subsequent experiments were done without PCNA.

The N^2-alkylG adducts caused some retardation of extension but relatively little compared with HIV-1 RT, pol T7$^-$, and human pols η and ι (28–30). With the highest concentration of pol κ, all of the primers were extended to mostly 34-mers and some full-length 36-mer products with the N^2-AnthG template; even with N^2-BPG about one-half of the primer was similarly extended. Generally the accumulation of products with only one base inserted was relatively low.

Steady-state Kinetics of dNTP Incorporation by pol κ Opposite G and N^2-G Adducts—Preliminary analyses with single dNTPs indicated that dCTP, dTTP, and dGTP were inserted opposite all of the N^2-alkylG adducts and dATP was not. Steady-state kinetic analyses were done with varying concentrations of dCTP, dTTP, and dGTP under conditions that favor only the incorporation of a single base and the oligomer substrate is not depleted (Table 2). One possibility that cannot be dismissed, in the absence of sequence analysis of larger products, is that the (limited) dGTP insertion occurs opposite the C base 5′ to the adduct (Table 1).

Several points are in order. The K_m values for dCTP, the correct nucleotide, are higher with pol κ than we have measured under similar conditions for several replicative DNA polymerases (28, 34, 39–43) but similar to those for *Sulfolobus solfataricus* Dpo4 (44, 45) and human pol η (29) and much lower than for human pol ι (30). The misinsertion ratios were low for pol κ, even with the bulkiest adducts, where the proclivity to misinsert dGTP and dTTP was similar to that seen for G itself.

TABLE 3
Steady-state kinetic parameters for next base extension from G (or N^2-G adduct):C (or T) template·primer termini by human pol κ

Base-pair at 3′ primer termini (template·primer)	Extension with dGTP (the next correct nucleotide against template C)			
	K_m	k_{cat}	k_{cat}/K_m	f_{ext}
	μM	s^{-1}	$mM^{-1}\ s^{-1}$	Misextension efficiency
G·C	5.7 ± 0.6	0.23 ± 0.01	40	1
G·T	97 ± 11	0.027 ± 0.001	0.28	0.007
N^2-MeG·C	6.5 ± 0.8	0.046 ± 0.002	7.1	1
N^2-MeG·T	130 ± 10	0.012 ± 0.001	0.092	0.013
N^2-EtG·C	5.8 ± 0.7	0.25 ± 0.01	43	1
N^2-EtG·T	100 ± 10	0.020 ± 0.001	0.20	0.0049
N^2-IbG·C	6.4 ± 0.7	0.21 ± 0.01	33	1
N^2-IbG·T	37 ± 3	0.011 ± 0.001	0.30	0.0091
N^2-BzG·C	16 ± 1	0.15 ± 0.01	9.4	1
N^2-BzG·T	180 ± 20	0.023 ± 0.001	0.13	0.014
N^2-NaphG·C	8.6 ± 0.9	0.10 ± 0.01	12	1
N^2-NaphG·T	130 ± 10	0.015 ± 0.001	0.12	0.01
N^2-AnthG·C	9.9 ± 0.7	0.19 ± 0.01	19	1
N^2-AnthG·T	140 ± 10	0.0066 ± 0.0001	0.047	0.0024
N^2-BPG·C	18 ± 3	0.058 ± 0.003	3.2	1
N^2-BPG·T	100 ± 10	0.0037 ± 0.0001	0.037	0.012

Another important point is that k_{cat}/K_m, the catalytic specificity, only decreased by one order of magnitude when going from G to the very bulky N^2-BPG.

Steady-state Kinetics of Next-base Extension Following G and N^2-G Adducts Paired with C or T—The literature reports a number of accounts of extension of pol κ past adducts paired with inserted bases, and the view has been presented that this function is more facile than insertion (26, 46, 47). Steady-state kinetic analysis was done with either C or T positioned opposite G or the N^2-alkylG adduct (Table 3).

The kinetic parameters were quantitatively similar to those measured for insertion reactions (Table 2). A strong tendency to extend the G/N^2-alkylG:C pairs was observed, relative to pairs with T. As in the case of insertion opposite N^2-alkylG adducts (Table 2), the decrease in k_{cat}/K_m was only one order of magnitude over the range from G to N^2-BPG. Thus, both insertion and extension are both relatively low error processes with pol κ.

Pre-steady-state Burst Kinetics of dCTP Incorporation Opposite G, N^2-AnthG, and N^2-BPG by pol κ—Steady-state kinetic parameters are useful in understanding DNA polymerases but are limited in the amount of information they can provide in terms of mechanistic details about catalysis (27). To our knowledge, pre-steady-state kinetic measurements have not been reported previously with pol κ, and analyses were done to characterize aspects of catalysis (Fig. 3).

For dCTP incorporation opposite G, clear burst kinetics was observed (Fig. 3). The shape of the burst is not as sharp as in the case of several of the highly replicative polymerases we have studied (34, 40, 45) and in human pol η (29). The "break" between the first cycle and the linear, steady-state phase is less pronounced and reminiscent of the patterns seen with *E. coli* pol I (Klenow fragment, exonuclease$^-$) and pol II (exonuclease$^-$) (39) (but more defined than seen with pol ι (30)). The patterns can be understood largely in the context of the rate of forward progress through the catalytic cycle relative to rates of release of the DNA substrate/product from the enzyme (4, 30).

The burst rates are modestly rapid, even with a bulky adduct present (N^2-AnthG) (Fig. 3). Even with the very bulky N^2-BPG adduct, a weak burst was observed. The observation of partial bursts with a system for the same oligonucleotide (as a function of having an adduct present) is evidence for the existence of an inactive polymerase·DNA (dNTP) complex, in equilibrium with the active form (48), although we have not done the trap experiments necessary to further define such a system (28, 48, 49).

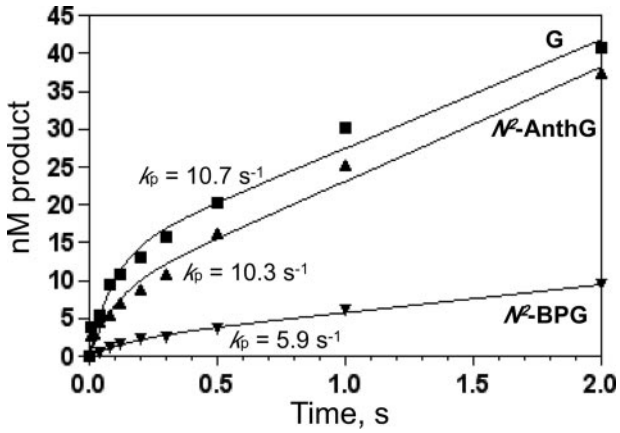

FIGURE 3. **Pre-steady-state burst kinetics of incorporation opposite G, N^2-AnthG, and N^2-BPG by human pol κ.** pol κ (17 nM) was incubated with 100 nM 24-mer/36-mer primer·template complex in a rapid quench-flow instrument and mixed with dCTP (and $MgCl_2$) to initiate reactions: 1 mM dCTP for the 24-mer/36-G-mer (■), 24-mer/36-N^2-AnthG-mer (▲), and 24-mer/36-N^2-BPG-mer (▼). The polymerization reactions were quenched with 0.3 M EDTA at the indicated time intervals, and product formation was determined following separation by gel electrophoresis and phosphorimaging. The data were fit to the burst equation, $y = A(1 - e^{-k_p t}) + k_{ss}t$, as described under "Experimental Procedures" (without normalization of k_{ss} for enzyme concentration in the equation). Pre-steady-state rates (k_p) were estimated: G-mer, k_p = 10.7 ± 3.2 s^{-1}, k_{ss} = 0.87 ± 0.08 s^{-1}; N^2-AnthG-mer, k_p = 10.3 ± 4.3 s^{-1}, k_{ss} = 0.92 ± 0.07 s^{-1}; N^2-BPG-mer, k_p = 5.9 ± 1.0 s^{-1}, and k_{ss} = 0.22 ± 0.01 s^{-1}.

The existence of a burst indicates that the slow step in steady-state catalysis occurs *after* formation of the product, *e.g.* product release (50). This is clearly the case for dCTP insertion opposite G and N^2-AnthG. With dCTP incorporation opposite N^2-BPG, both the burst rate and the steady-state rates are attenuated. We hypothesize that this phenomenon is the result of decreased rates of incorporation, not DNA release from the enzyme. We did not measure k_{off} rates in this work with pol κ, but in our experience with all other DNA polymerases we have not observed major changes in k_{off} or K_d due to DNA modification (4).

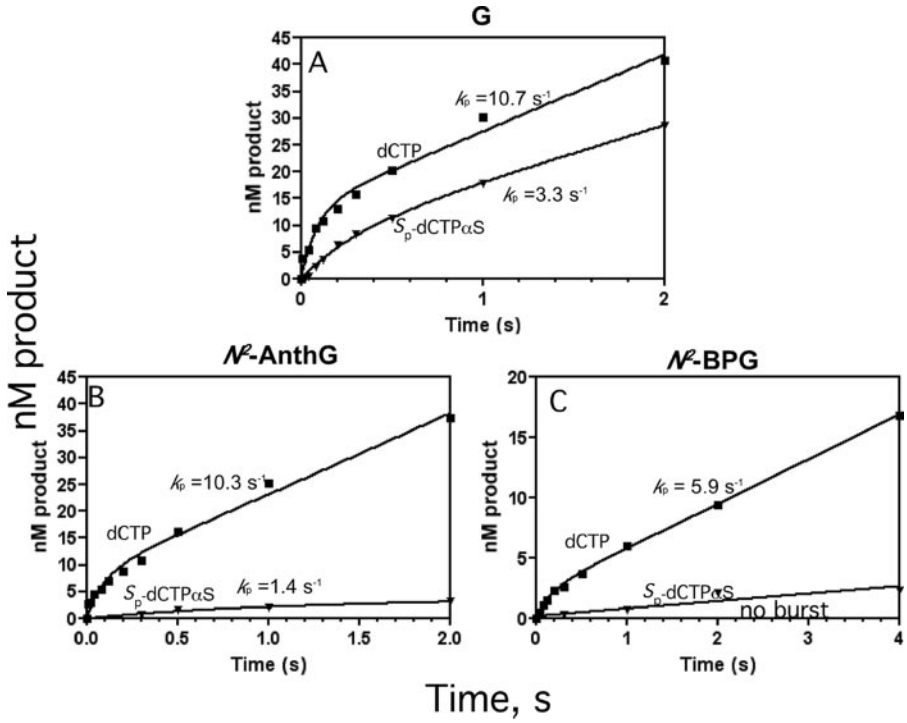

FIGURE 4. **Phosphorothioate analysis of pre-steady-state kinetics of nucleotide incorporation by human pol κ.** pol κ (17 nM) was incubated with 100 nM 24-mer/36-mer primer·template complexes (^{32}P-labeled primer) in a rapid quench-flow instrument and mixed with 1 mM dCTP (■) or (S_p)-dCTPαS (▼) to initiate reactions for the 24-mer/36-G-mer (*A*), 24-mer/36-N^2-Anth-mer (*B*), and 24-mer/36-N^2-BPG-mer (*C*). Pre-steady-state rates (k_p) were determined from the burst equation (Fig. 3), and *solid lines* represent the best fits. The following rates were estimated: *A*, dCTP, $k_p = 10.7 \pm 3.2\ s^{-1}$; ($S_p$)-dCTPαS, $k_p = 3.3 \pm 0.9\ s^{-1}$; *B*, dCTP, $k_p = 10.3 \pm 4.3\ s^{-1}$; ($S_p$)-dCTPαS, $k_p = 1.4 \pm 0.6\ s^{-1}$; *C*, dCTP, $k_p = 5.9 \pm 1.0\ s^{-1}$; ($S_p$)-dCTPαS, no burst (linear rate, $k = 0.05 \pm 0.01\ s^{-1}$).

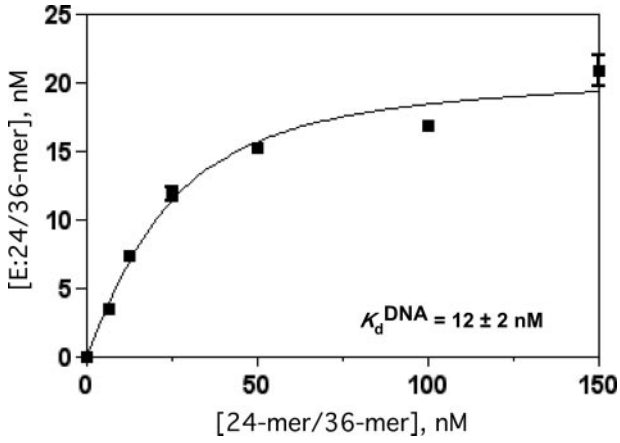

FIGURE 5. **Determination of K_d^{DNA} for human pol κ by active site titration.** pol κ (final nominal concentration, 120 nM) was incubated with varying 24-mer/36-G-mer (^{32}P-labeled) concentrations (■, 6–150 nM) and mixed with 1 mM dCTP to initiate the reaction. Reactions were quenched with EDTA after 0.2 s, and product formation was analyzed by gel electrophoresis and phosphorimaging. A plot of burst amplitudes *versus* total DNA concentration was fit to a quadratic equation (see "Experimental Procedures"), yielding an active site concentration of 21.1 ± 0.9 nM and $K_d^{DNA} = 11.5 \pm 2.3$ nM.

Phosphorothioate Analysis of dCTP Incorporation Opposite G, N^2-AnthG, and N^2-BPG Adducts by pol κ—One approach to further delineation of aspects of catalysis by DNA polymerases is the use of sulfur/oxygen elemental effects on rates. The principle is similar to that utilized with kinetic isotope effects, in that the substitution of an α-oxygen of a dNTP with sulfur decreases the electronegativity and makes bond breakage more difficult. If this is a slow step in the reaction, then the overall reaction will be slowed (51, 52). This is a simplistic interpretation and, as with many aspects of kinetic hydrogen isotope effects, the detailed interpretation of the extent of the changes has some differences in interpretation (53).

When these studies were done with pol κ, only a relatively small difference in burst rates was observed in incorporation of dCTP opposite G (Fig. 4). The difference (the thio effect) was much greater in the case of dCTP incorporation opposite N^2-AnthG and N^2-BPG (Fig. 4). For the respective two adducts, the thio effects were 7 and ~120.

Active Site Titration and Estimation of the Productive K_d^{DNA} for pol κ—The observation of burst kinetics (Figs. 3 and 4) allowed for the estimation of several parameters using kinetic means. One analysis is the "active site" titration (Fig. 5). In this experiment, the K_d for DNA was estimated to be 12 nM (Fig. 5). This value is similar to that estimated for pol η (29) and most of the replicative DNA polymerases (34, 39, 40) but ~5-fold less than for pol ι (30) or, interestingly, bovine pol δ (34).

Determination of K_d^{dCTP} (dCTP Incorporation) by pol κ—The initial analyses of pre-steady-state kinetics (Fig. 3) provide estimates of the rate of burst phase (k_p), but this requires extrapolation to high concentration to estimate k_{pol}. These experiments were done (Fig. 6). The k_{pol} values for dCTP incorporation opposite G and the bulky adduct N^2-AnthG were identical, and the K_d^{dCTP} value for incorporation opposite N^2-AnthG was ~2-fold higher than opposite G.

The K_d^{dNTP} values are much higher than reported for processive DNA polymerases, *i.e.* 1–4 μM (34), but are similar to those reported for other translesion DNA polymerases (29, 30, 54). The adduct does not make a large difference in the K_d^{dNTP}. Another point of interest is that the K_d^{dNTP} values are much higher than the K_m values reported for these reactions (Table 2), and the specific contribution of K_d to the parameter K_m is not clear.

Primer Extension (All Four dNTPs) Opposite N^2-EtG and N^2,N^2-diMeG by Human pol δ and κ—pol ι appears to utilize Hoogsteen base pairing instead of (or at least in addition to) the classic Watson-Crick mode (55, 56). One way of analyzing the ability of polymerases to "replace" Watson-Crick hydrogen bonding with a Hoogsteen mode is to compare the abilities to insert N^2,N^2-diMeG relative to N^2-EtG (30), because these two lesions are nearly isosteric, but N^2,N^2-diMeG eliminates the N2 hydrogen atom from a Watson-Crick pairing mode. When

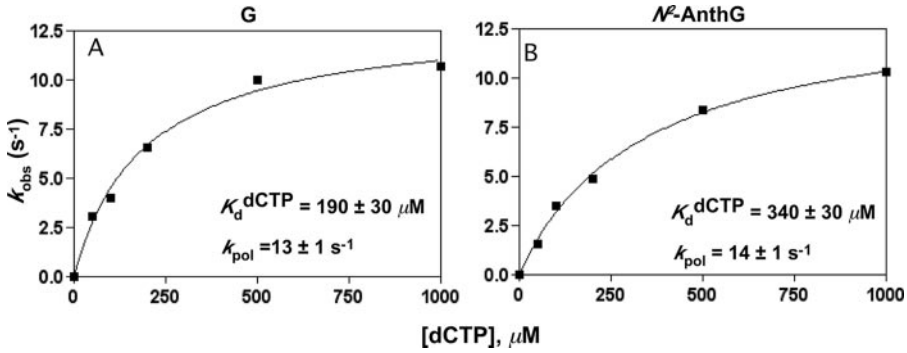

FIGURE 6. **Estimation of K_d^{dCTP} for human pol κ by pre-steady-state burst rate dependence on dCTP concentration.** pol κ (17 nM) was incubated with 100 nM 24-mer/36-mer primer·template complex (^{32}P-labeled) in a rapid quench-flow instrument and mixed with varying dCTP concentrations (■, 50–1000 μM) to initiate reactions. Reactions were quenched with EDTA, and product formation was analyzed following electrophoresis and phosphorimaging. A plot of burst rates (k_{obs}) *versus* [dCTP] was fit to a hyperbolic equation (see "Experimental Procedures"). *A*, G (unmodified): k_{pol} (extrapolated maximum rate of nucleotide incorporation) = 13.1 ± 0.7 s^{-1} and K_d^{dCTP} = 190 ± 30 μM; *B*, N^2-AnthG: k_{pol} = 13.8 ± 0.6 s^{-1} and K_d^{dCTP} = 340 ± 30 μM.

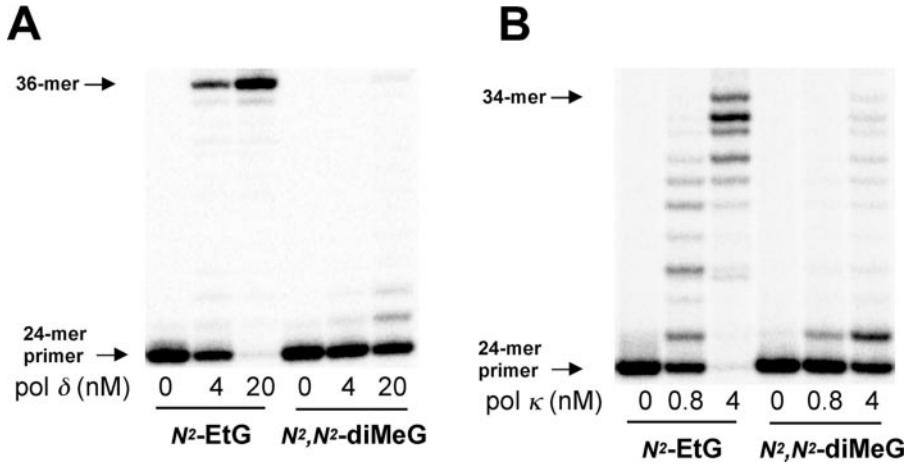

FIGURE 7. **Extension of ^{32}P-labeled 24-mer primer complexed with templates containing N^2-EtG and N^2,N^2-diMeG by human pol δ and κ.** The ^{32}P-labeled 24-mer primer was annealed with 36-mer templates (Table 1) containing an N^2-EtG or N^2,N^2-diMeG placed at the 25th position from the 3′-end. The ^{32}P-labeled 24-mer primer was extended in the presence of all four dNTPs for 15 min with varying amounts of pol δ (0–20 nM, with excess PCNA (34)) and pol κ (0–4 nM) and a constant concentration of DNA substrate (100 nM primer·template), as indicated. The reaction products were analyzed by denaturing gel electrophoresis with subsequent phosphorimaging. *A*, pol δ-PCNA; *B*, pol κ.

DISCUSSION

A series of kinetic studies were done with purified recombinant human pol κ and a defined set of oligonucleotides varying only in the size of a substitution at the guanine N2 atom, with the only changes being in the associated steric bulk, hydrophobicity, and electronic properties. Although the view has been advanced that the role of pol is to extend primers past a base incorporated opposite an adduct, the quantitative evidence to support this view is very limited. We have used a number of more quantitative approaches to address this issue, at least within the context of the set of N^2-G modifications. The results indicate that pol κ is relatively proficient in inserting dCTP opposite the modified guanines as well as extending pairs, as demonstrated using steady-state and pre-steady-state approaches. Although the catalytic specificity constant, k_{cat}/K_m, has some deficiencies in describing enzyme reactions, it is a useful first approximation of enzyme efficiency and provides a basis for understanding polymerase function as a function of molecular size of adducts. Such plots for incorporation (dCTP, dTTP, and dGTP) (Fig. 8*A*) and extension beyond N^2-G adducts (paired with C or T) (Fig. 8*B*) can be used as the basis for several conclusions: (i) pol κ is more efficient than (human) pol η or pol ι in incorporating dCTP opposite large N^2-G adducts (N^2-AnthG and N^2-BPG) (29, 30); (ii) the preference for insertion of dCTP relative to other dNTPs is similar to that of pol η (and better with the bulkier adducts) (29) and much better than that of pol ι (30); (iii) pol κ is much less influenced by adduct size than any other DNA polymerases studied in similar systems (28–30); and (iv) similar conclusions can be drawn about extension beyond N^2-G adduct:C pairs (Fig. 8*B*). The conclusions about insertion are reinforced by the more qualitative results of the "run-on" experiments (Fig. 2) and the burst kinetics observed in the pre-steady-state analyses (Figs. 3 and 4). Overall, these studies provide a better understanding of the action of pol κ, at least with N^2-alkyl- and -aralkylG adducts.

these experiments were done in another setting (30), human pol η did not show activity with N^2,N^2-diMeG, but human pol ι did (30), consistent with the proposal that Hoogsteen base pairing is operative with pol ι (55, 56).

When these experiments were done with pol δ, little incorporation opposite N^2,N^2-diMeG was observed (Fig. 7*A*). With pol κ, some incorporation opposite N^2,N^2-diMeG and extension were observed (Fig. 7*B*), indicating that pol κ may have some limited capability to utilize non-Watson-Crick pairing modes.

The system was evaluated in more detail, using steady-state kinetic analysis (Table 4). The k_{cat}/K_m for incorporation of dCTP opposite N^2,N^2-diMeG was 47-fold lower than for N^2-EtG with pol κ, compared with a 2,000-fold difference with pol δ/PCNA. The major misincorporation for pol δ was dATP and that for pol κ was dTTP. The misincorporation showed less attenuation due to removal of the N2 hydrogen. These results are consistent with the view of a finite but limited role for non-Watson-Crick pairing with pol κ.

Although the view has been advanced that the role of pol κ is to extend primers from a base incorporated opposite an adduct by other polymerases, the quantitative evidence to support this view is very limited in that it has been tested only with some adducts such as 3′ T of the T-T dimer and O^6-MeG (20, 25), and

TABLE 4
Comparison of steady-state kinetic parameters for one-base incorporation opposite N^2-EtG and N^2,N^2-diMeG by human pol κ and δ

Polymerase	Template·dNTP	K_m	k_{cat}	k_{cat}/K_m	Difference of k_{cat}/K_m, compared to N^2-EtG	f
		μM	s^{-1}	$mM^{-1}\,s^{-1}$	*-fold*	*Misinsertion ratio*
Pol κ	N^2-EtG·dCTP	22 ± 2	0.36 ± 0.01	16.4		1
	N^2,N^2-diMeG·dCTP	780 ± 100	0.27 ± 0.01	0.35	47-fold lower	1
	N^2-EtG·dTTP	1600 ± 600	0.15 ± 0.03	0.094		0.0057
	N^2,N^2-diMeG·dTTP	2000 ± 200	0.14 ± 0.01	0.07	No significant difference	0.2
Pol δ (with PCNA)	N^2-EtG·dCTP	3.5 ± 0.6	0.014 ± 0.001	4.0		1
	N^2,N^2-diMeG·dCTP	1400 ± 600	0.0029 ± 0.0006	0.002	2000-fold lower	1
	N^2-EtG·dATP	610 ± 80	0.012 ± 0.001	0.019		0.0048
	N^2,N^2-diMeG·dATP	360 ± 60	0.0018 ± 0.0001	0.005	4-fold lower	2.5

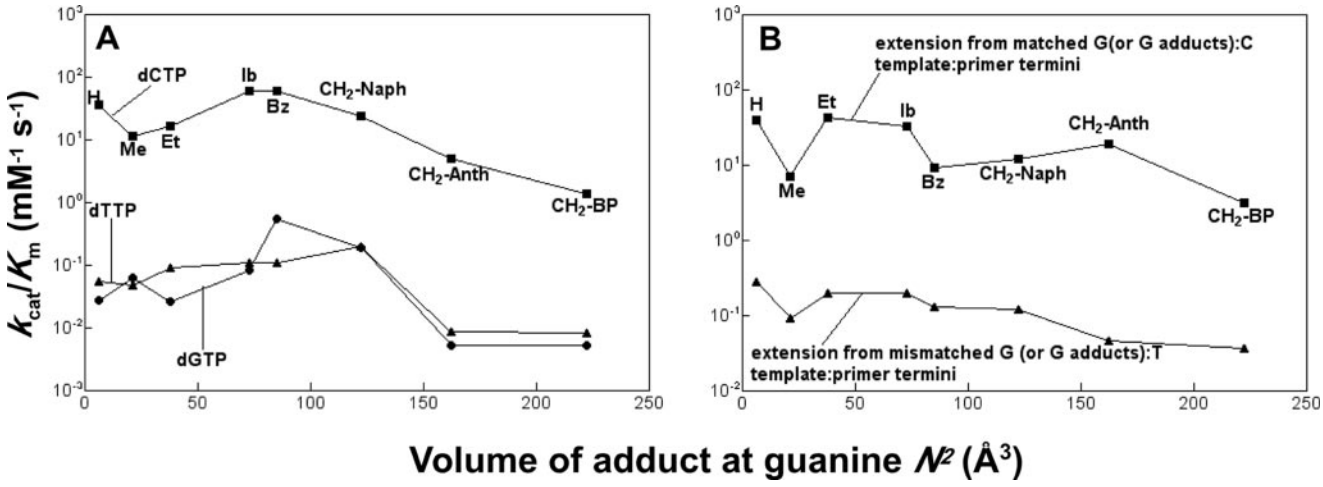

FIGURE 8. **Effect of the volume of adduct at the guanine N2 atom on catalytic efficiency (k_{cat}/K_m) for dCTP incorporation opposite N^2-G adducts by human pol κ.** *A*, molecular volumes (Å^3) of adducts at the guanine N2 atom were calculated using the program Chem3D (version 7.0), based on the Connolly surface algorithm (57), and plotted against k_{cat}/K_m values (Table 2) for dCTP (■), dATP (●), and dTTP (▲) incorporation for various N^2-G adducts by pol κ. *B*, molecular volumes (Å^3) of adducts at the guanine N2 atom are plotted against k_{cat}/K_m values (Table 3) for next-base extension (with dGTP) from matched G (or N^2-G adducts):C template·primer termini (■) or mismatched G (or N^2-G adducts):T template·primer termini (▲) by pol κ.

no direct comparisons have been made for extension ability with other translesion polymerases. The k_{cat}/K_m values for next-base extension can be compared with those for base incorporation opposite various N^2-alkylG adducts by each polymerase (Supplemental Fig. S2), and the plots clearly indicate that pol κ is almost as efficient in incorporation opposite lesion as in extension. pol η is rather slightly more efficient in extension than incorporation. Interestingly, pol ι is less efficient in extension than incorporation with the mismatched G:T base pair, but the opposite pattern is observed with the matched G:C base pair.

The comparisons of the abilities of pol κ to insert opposite (and copy past) N^2-EtG and N^2,N^2-diMeG (Fig. 7 and Table 4) provide some insight into the mode of binding of nucleotide triphosphates. Moderate loss of efficiency and fidelity opposite N^2,N^2-diMeG (*versus* N^2-EtG) indicates that the error-free bypass opposite N^2-G adducts (at least N^2-EtG) by pol κ may depend considerably on the Watson-Crick pairing, in agreement with a recent report (58). However, the dependence on the third hydrogen bonding capability during bypass by pol κ is much less than pols δ and η (30), and pol κ exhibited some activity toward N^2,N^2-diMeG, at least more than human pol δ/PCNA. Binding of dCTP opposite N^2,N^2-diMeG does not involve classic Watson-Crick pairing, because no N2 hydrogen is available (at least with this atom). pol ι, for which structural evidence exists to support a Hoogsteen pairing mode (55, 56), is proficient in insertion opposite N^2,N^2-diMeG (30). Our present results suggest that pol κ has some limited, but not extensive, ability to utilize non-Watson-Crick modes of pairing or other possible supportive interactions, which might be specialized for N^2-bulk itself in the minor groove side. A crystal structure of the core of human pol κ has been published (8) but without DNA. Models have been made with DNA inserted into the available structure, based on the available structures of yeast pol η and *S. solfataricus* Dpo4 (8), although the conclusions cannot support or refute the possibility of non-Watson Crick pairing for pol κ. We also note a recent report that a steric gate residue (Phe) has a critical role in bypass of some N^2-G adducts by *E. coli* DinB (DNA polymerase IV), an apparent orthologue of human pol κ (59).

The available results support the general DNA polymerase mechanism shown in Fig. 9. Some support for the contribution of a non-productive polymerase-DNA (dNTP) complex is provided by the partial bursts seen with the N^2-G adducts in Fig. 3 (48), although further experiments are to prove this. In a typical steady-state experiment with excess oligonucleotide (*e.g.* Table 2), a step following product formation must be rate-limiting, at least for incorporation opposite G and the less bulky adducts, because of the burst kinetics (Fig. 3). Although we did not measure k_{off} rates for pol κ, we hypothesize that step 7 (of Fig. 9) is probably rate-limiting and has a major influence on k_{cat}, as with most DNA polymerases (27, 37). Within the catalytic cycle itself

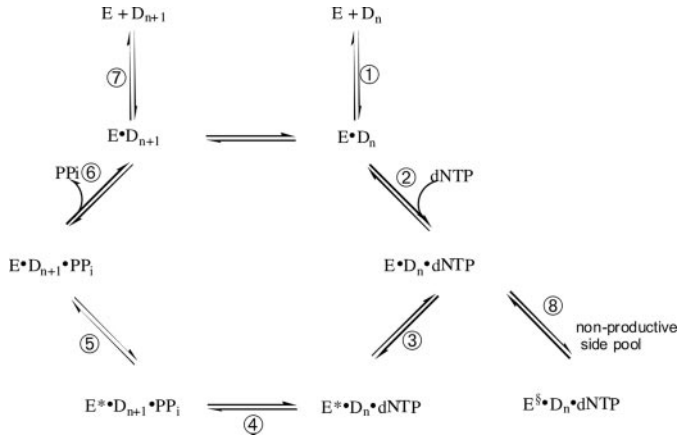

FIGURE 9. **General kinetic mechanism for DNA polymerization.** Individual steps are *numbered* and discussed in the text. E = pol (K), D_n = DNA substrate, E^* = conformationally altered polymerase, $E^§$ = nonproductive conformation of polymerase, D_{n+1} = DNA extended by one base, and PP_1 = pyrophosphate.

(steps **2**-**6** of Fig. 9), either step **3** (a proposed conformational change) or **4** (phosphodiester bond formation) is rate-limiting. Step **3** has precedent in studies with other DNA polymerases, although its identity is controversial (60, 61). Some key experiments to establish the existence of step **3** have not been done with pol κ, *e.g.* pulse-chase *versus* pulse-quench (60, 62). The elemental influence on rates (*i.e.* thio effects, Fig. 4) are not without controversy regarding their interpretation (53, 61, 63, 64). However, the results are quite clear (Fig. 4), and the patterns resemble those observed for several other DNA polymerases, *i.e.* low thio effects (≤3) for normal incorporation and high thio effects for (≥7) for misincorporation or incorporation of the "right" dNTP opposite an adduct (39, 40, 65, 66). The most direct interpretation of such results, such as these, is that a "non-chemical" step is rate-limiting for normal base incorporation (step **3** of Fig. 9) but, as the reaction becomes more difficult, then step **4** becomes limited. Such an interpretation has been challenged on the basis that the sulfur substitution can change steric influences as well as electronic (53, 61, 63, 64), although the point has been made that any strong perturbation of rates by thio substitution is indicative of an effect on step **4** (42, 63), and we currently continue to favor this interpretation for pol κ, based on the very dramatic effects (Fig. 4, *B* and *C*). Thus, step **3** is probably most rate-limiting for normal incorporation (Fig. 4*A*) (and this evidence indirectly argues for the existence of step **3**), but step **4** becomes more rate-limiting as the size of the DNA adduct increases. Another point is that the steady-state rates with the largest adducts (*e.g.* N^2-BPG in Fig. 3) are slower and probably reflect step **4** more than in the case of normal base incorporation, in which k_{cat} is more dominated by events following product formation.

The availability of a collection of kinetic and other parameters for full-length recombinant human pols η, ι, and κ now permits several comparisons (29, 30). k_{pol} (or at least k_p, estimated at a single high dCTP concentration) for pol κ (13 s^{-1}) is intermediate between pols η and ι (40 and 4 s^{-1}, respectively) for incorporation opposite G but is much better with pol κ for large adducts than the other polymerases, *e.g.* 6 s^{-1} for pol κ with N^2-BPG, compared with 0.24 s^{-1} for pol η. Much discussion has been made of the distributive nature of translesion DNA polymerases compared with the processive behavior of the replicative polymerases (26, 67). However, our own results have generally shown that the translesion polymerases have DNA affinities similar to the replicative polymerases (34); *e.g.* the K_d^{DNA} for pol κ is 12 nM (Fig. 5). The major difference is in the rates of forward progress (*i.e.* k_{pol}), as opposed to k_{off}, and processivity can be viewed as the ratio k_{pol}/k_{off}, to a first approximation. All three of the translesion polymerases have high K_d^{dCTP} values, similar to Dpo4 (54). pol η showed no real thio effect with any of the adducts (29) and pol ι, like pol κ, showed a low effect for normal incorporation and relatively high effects with dCTP incorporation opposite the adducts.

The data sets available for these N^2-G adducts (28–30) can be summarized and compared. The replicative polymerases ($T7^-$, HIV-1 RT, and human pol δ/PCNA) are very efficient in normal incorporation but very sensitive to even a small substitution at the N2 atom of G. The incorporation that does occur with large adducts is with dATP. Human pol δ is actually more tolerant of size than the two viral polymerases (HIV-1 RT and $T7^-$). The Y-family translesion polymerases are less efficient but more tolerant of the adduct size (or other associated properties, *i.e.* hydrophobicity and electronic effects). pol η shows the highest fidelity with N^2-G adducts up to N^2-NaphG (*i.e.* inserting dCTP opposite) but loses the fidelity with larger adducts, whereas pol κ has the highest fidelity throughout the whole series (Fig. 8*A*). pol κ was clearly the most tolerant of the larger adducts.

Finally, the available information about N^2-G adducts can be considered in a more general view with what happens in mammalian systems, based on the work now available with human pols δ, η, ι, and κ (29, 30). With small N^2-G lesions (Me or Et), pol δ can bypass these in an error-free manner (30). With larger lesions, pol δ stalls and one of the translesion polymerases is more effective. With an N^2-G lesion smaller than N^2-NaphG, any of these three polymerases can catalyze bypass replication. pol ι is error-prone (30) and pols η and κ are relatively error-free. With adducts as large as or larger than N^2-AnthG, pol η or κ is active, the former being error-prone (29) and the latter being relatively error-free (Fig. 8). The base sequence context can be a major factor for error-free or error-prone bypass in this step, in that pol κ shows 3 orders of magnitude of differences in V_{max} (k_{cat})/K_m of dCTP incorporation opposite (+)-*trans-anti*-benzo[*a*]pyrene diol epoxide-modified-N^2-G in different sequences (14), although having no available information for pol η. The possible role of pol κ in efficient and error-free bypass of N^2-BPDE-modified-G has also been suggested by quantitative analysis in mammalian cells (68). Because the rates of polymerization are not competitive with dissociation, the translesion polymerases have distributive behavior and leave the DNA, being replaced soon by pol δ.

These studies have a reductionist character by their very nature, and caution needs to be used in extrapolation to other adducts. However, we are of the opinion that systematic studies of this type are necessary to understand catalysis by these polymerases, in that the battery of DNA adducts already studied (with pol κ (9–21)) varies considerably in positional, steric, and electronic properties and that any quantitative conclusions are

difficult. Finally, the systems are undoubtedly more complex in cells. Still other DNA polymerases are present, and the contributions of accessory proteins cannot be ignored. In this regard, we have utilized PCNA with pol δ (30, 34) but have uniformly found no stimulation of activity, in studies with short oligonucleotides, with human pols η, ι, and κ (29, 30) (see above), and Gerlach *et al.* (10) also reported a lack of effect of PCNA on pol κ. However, the situation with large pieces of DNA and *in vivo* may differ, and specific translational modifications of PCNA (ubiquitination and sumoylation) have been investigated for their effects (69–71), although doing quantitative *in vitro* investigations with such systems remains a challenge.

In summary, the enzymatic properties of the recombinant human translesion DNA polymerase pol κ have been studied. Although the amounts of the full-length protein available were very limited, it was possible to carry out a number of the most relevant steady-state and pre-steady-state experiments because of the high sensitivity available using ^{32}P-labeled substrates. Studies with a set of defined N^2-G adducts varying only in size were utilized, and the quantitative results allow the conclusion that pol κ catalyzes relatively efficient and high fidelity incorporation of dCTP opposite these adducts, being rather refractory to bulk size. Insertion and extension beyond a pair proceed with similar efficiency. The contributions of different steps in the catalytic cycle of pol κ changes with the size of the N^2-G lesion, and some involvement of non-Watson-Crick base pairing of dCTP with the N^2-G adducts may occur. Finally, we conclude that pol κ may be considered to be the most efficient and accurate enzyme for bypass of bulky N^2-guanine minor groove DNA adducts, at least among those considered here.

Acknowledgment—We thank K. Trisler for assistance in preparation of the manuscript.

REFERENCES

1. Friedberg, E. C., Walker, G. C., Siede, W., Wood, R. D., Schultz, R. A., and Ellenberger, T. (2006) *DNA Repair and Mutagenesis*, 2nd Ed., American Society of Microbiology Press, Washington, D. C.
2. Ramos, K. S., and Moorthy, B. (2005) *Drug Metab. Rev.* **37,** 595–610
3. Goodman, M. F. (1997) *Proc. Natl. Acad. Sci. U. S. A.* **94,** 10493–10495
4. Guengerich, F. P. (2006) *Chem. Rev.* **106,** 420–452
5. Goodman, M. F. (2002) *Annu. Rev. Biochem.* **71,** 17–50
6. Gerlach, V. L., Aravind, L., Gotway, G., Schultz, R. A., Koonin, E. V., and Friedberg, E. C. (1999) *Proc. Natl. Acad. Sci. U. S. A.* **96,** 11922–11927
7. Ogi, T., Kato, T., Jr., Kato, T., and Ohmori, H. (1999) *Genes Cells* **4,** 607–618
8. Uljon, S. N., Johnson, R. E., Edwards, T. A., Prakash, S., Prakash, L., and Aggarwal, A. K. (2004) *Structure* (*Cambridge*) **12,** 1395–1404
9. Zhang, Y., Yuan, F., Wu, X., Wang, M., Rechkoblit, O., Taylor, J. S., Geacintov, N. E., and Wang, Z. (2000) *Nucleic Acids Res.* **28,** 4138–4146
10. Gerlach, V. L., Feaver, W. J., Fischhaber, P. L., and Friedberg, E. C. (2001) *J. Biol. Chem.* **276,** 92–98
11. Rechkoblit, O., Zhang, Y., Guo, D., Wang, Z., Amin, S., Krzeminsky, J., Louneva, N., and Geacintov, N. E. (2002) *J. Biol. Chem.* **277,** 30488–30494
12. Zhang, Y., Wu, X., Guo, D., Rechkoblit, O., and Wang, Z. (2002) *DNA Repair* (*Amst.*) **1,** 559–569
13. Suzuki, N., Ohashi, E., Kolbanovskiy, A., Geacintov, N. E., Grollman, A. P., Ohmori, H., and Shibutani, S. (2002) *Biochemistry* **41,** 6100–6106
14. Huang, X., Kolbanovskiy, A., Wu, X., Zhang, Y., Wang, Z., Zhuang, P., Amin, S., and Geacintov, N. E. (2003) *Biochemistry* **42,** 2456–2466
15. Yasui, M., Suzuki, N., Miller, H., Matsuda, T., Matsui, S., and Shibutani, S. (2004) *J. Mol. Biol.* **344,** 665–674
16. Suzuki, N., Yasui, M., Geacintov, N. E., Shafirovich, V., and Shibutani, S. (2005) *Biochemistry* **44,** 9238–9245
17. Suzuki, N., Itoh, S., Poon, K., Masutani, C., Hanaoka, F., Ohmori, H., Yoshizawa, I., and Shibutani, S. (2004) *Biochemistry* **43,** 6304–6311
18. Ohashi, E., Bebenek, K., Matsuda, T., Feaver, W. J., Gerlach, V. L., Friedberg, E. C., Ohmori, H., and Kunkel, T. A. (2000) *J. Biol. Chem.* **275,** 39678–39684
19. Levine, R. L., Miller, H., Grollman, A., Ohashi, E., Ohmori, H., Masutani, C., Hanaoka, F., and Moriya, M. (2001) *J. Biol. Chem.* **276,** 18717–18721
20. Haracska, L., Prakash, L., and Prakash, S. (2002) *Proc. Natl. Acad. Sci. U. S. A.* **99,** 16000–16005
21. Singer, B., Medina, M., Zhang, Y., Wang, Z., Guliaev, A. B., and Hang, B. (2002) *Biochemistry* **41,** 1778–1785
22. O-Wang, J., Kawamura, K., Tada, Y., Ohmori, H., Kimura, H., Sakiyama, S., and Tagawa, M. (2001) *Cancer Res.* **61,** 5366–5369
23. Schenten, D., Gerlach, V. L., Guo, C., Velasco-Miguel, S., Hladik, C. L., White, C. L., Friedberg, E. C., Rajewsky, K., and Esposito, G. (2002) *Eur. J. Immunol.* **32,** 3152–3160
24. Bavoux, C., Hoffmann, J. S., and Cazaux, C. (2005) *Biochimie* (*Paris*) **87,** 637–646
25. Washington, M. T., Johnson, R. E., Prakash, L., and Prakash, S. (2002) *Proc. Natl. Acad. Sci. U. S. A.* **99,** 1910–1914
26. Prakash, S., Johnson, R. E., and Prakash, L. (2005) *Annu. Rev. Biochem.* **74,** 317–353
27. Johnson, K. A. (1993) *Annu. Rev. Biochem.* **62,** 685–713
28. Choi, Y.-J., and Guengerich, F. P. (2004) *J. Biol. Chem.* **279,** 19217–19229
29. Choi, J.-Y., and Guengerich, F. P. (2005) *J. Mol. Biol.* **352,** 72–90
30. Choi, J.-Y., and Guengerich, F. P. (2006) *J. Biol. Chem.* **281,** 12315–12324
31. Borer, P. N. (1975) in *Handbook of Biochemistry and Molecular Biology* (Fasman, G. D., ed) pp. 589–590, 3rd Ed., CRC Press, Cleveland, OH
32. Wray, W., Boulikas, T., Wray, V. P., and Hancock, R. (1981) *Anal. Biochem.* **118,** 197–203
33. Fien, K., and Stillman, B. (1992) *Mol. Cell Biol.* **12,** 155–163
34. Einolf, H. J., and Guengerich, F. P. (2000) *J. Biol. Chem.* **275,** 16316–16322
35. Goodman, M. F., Creighton, S., Bloom, L. B., and Petruska, J. (1993) *Crit. Rev. Biochem. Mol. Biol.* **28,** 83–126
36. Patel, S. S., Wong, I., and Johnson, K. A. (1991) *Biochemistry* **30,** 511–525
37. Johnson, K. A. (1995) *Methods Enzymol.* **249,** 38–61
38. Haracska, L., Unk, I., Johnson, R. E., Phillips, B. B., Hurwitz, J., Prakash, L., and Prakash, S. (2002) *Mol. Cell Biol.* **22,** 784–791
39. Lowe, L. G., and Guengerich, F. P. (1996) *Biochemistry* **35,** 9840–9849
40. Furge, L. L., and Guengerich, F. P. (1997) *Biochemistry* **36,** 6475–6487
41. Woodside, A. M., and Guengerich, F. P. (2002) *Biochemistry* **41,** 1027–1038
42. Zang, H., Harris, T. M., and Guengerich, F. P. (2005) *J. Biol. Chem.* **280,** 1165–1178
43. Zang, H., Harris, T. M., and Guengerich, F. P. (2005) *Chem. Res. Toxicol.* **18,** 389–400
44. Zang, H., Goodenough, A. K., Choi, J.-Y., Irminia, A., Loukachevitch, L. V., Kozekov, I. D., Angel, K. C., Rizzo, C. J., Egli, M., and Guengerich, F. P. (2005) *J. Biol. Chem.* **280,** 29750–29764
45. Zang, H., Irminia, A., Choi, J.-Y., Angel, K. C., Loukachevitch, L. V., Egli, M., and Guengerich, F. P. (2006) *J. Biol. Chem.* **281,** 2358–2372
46. Washington, M. T., Minko, I. G., Johnson, R. E., Wolfle, W. T., Harris, T. M., Lloyd, R. S., Prakash, S., and Prakash, L. (2004) *Mol. Cell Biol.* **24,** 5687–5693
47. Wolfle, W. T., Johnson, R. E., Minko, I. G., Lloyd, R. S., Prakash, S., and Prakash, L. (2006) *Mol. Cell Biol.* **26,** 381–386
48. Furge, L. L., and Guengerich, F. P. (1999) *Biochemistry* **38,** 4818–4825
49. Suo, Z., and Johnson, K. A. (1998) *J. Biol. Chem.* **273,** 27259–27267
50. Johnson, K. A. (2003) in *Kinetic Analysis of Macromolecules: A Practical Approach* (Johnson, K. A., ed) pp. 1–18, Oxford University Press, Oxford, UK
51. Mizrahi, V., Henrie, R. N., Marlier, J. F., Johnson, K. A., and Benkovic, S. J. (1985) *Biochemistry* **24,** 4010–4018
52. Kuchta, R. D., Mizrahi, V., Benkovic, P. A., Johnson, K. A., and Benkovic,

S. J. (1987) *Biochemistry* **26,** 8410–8417
53. Herschlag, D., Piccirilli, J. A., and Cech, T. R. (1991) *Biochemistry* **30,** 4844–4854
54. Fiala, K. A., and Suo, Z. (2004) *Biochemistry* **43,** 2106–2115
55. Nair, D. T., Johnson, R. E., Prakash, S., Prakash, L., and Aggarwal, A. K. (2004) *Nature* **430,** 377–380
56. Nair, D. T., Johnson, R. E., Prakash, L., Prakash, S., and Aggarwal, A. K. (2005) *Structure* (*Cambridge*) **13,** 1569–1577
57. Connolly, M. L. (1993) *J. Mol. Graph.* **11,** 139–141
58. Wolfle, W. T., Washington, M. T., Kool, E. T., Spratt, T. E., Helquist, S. A., Prakash, L., and Prakash, S. (2005) *Mol. Cell Biol.* **25,** 7137–7143
59. Jarosz, D. F., Godoy, V. G., Delaney, J. C., Essigmann, J. M., and Walker, G. C. (2006) *Nature* **439,** 225–228
60. Joyce, C. M., and Benkovic, S. J. (2004) *Biochemistry* **43,** 14317–14324
61. Showalter, A. K., and Tsai, M. D. (2002) *Biochemistry* **41,** 10571–10576
62. Fiala, K. A., and Suo, Z. (2004) *Biochemistry* **43,** 2116–2125
63. Polesky, A. H., Dahlberg, M. E., Benkovic, S. J., Grindley, N. D. F., and Joyce, C. M. (1992) *J. Biol. Chem.* **267,** 8417–8428
64. Zhong, X., Patel, S. S., Werneburg, B. G., and Tsai, M. D. (1997) *Biochemistry* **36,** 11891–11900
65. Eger, B. T., and Benkovic, S. J. (1992) *Biochemistry* **31,** 9227–9236
66. Furge, L. L., and Guengerich, F. P. (1998) *Biochemistry* **37,** 3567–3574
67. Hübscher, U., Maga, G., and Spadari, S. (2002) *Annu. Rev. Biochem.* **71,** 133–163
68. Avkin, S., Goldsmith, M., Velasco-Miguel, S., Geacintov, N., Friedberg, E. C., and Livneh, Z. (2004) *J. Biol. Chem.* **279,** 53298–53305
69. Ogi, T., Kannouche, P., and Lehmann, A. R. (2005) *J. Cell Sci.* **118,** 129–136
70. Haracska, L., Torres-Ramos, C. A., Johnson, R. E., Prakash, S., and Prakash, L. (2004) *Mol. Cell Biol.* **24,** 4267–4274
71. Watanabe, K., Tateishi, S., Kawasuji, M., Tsurimoto, T., Inoue, H., and Yamaizumi, M. (2004) *EMBO J.* **23,** 3886–3896

Translesion Synthesis across Bulky N^2-Alkyl Guanine DNA Adducts by Human DNA Polymerase κ

Jeong-Yun Choi, Karen C. Angel and F. Peter Guengerich

J. Biol. Chem. 2006, 281:21062-21072.
doi: 10.1074/jbc.M602246200 originally published online June 1, 2006